Supplementary Information

Induced Circular Dichroism of monoatomic anions: Silica-assisted chiral environment transfer from molecular assembled nanohelices to halide ions

Yutaka Okazaki,[a] Naoya Ryu,[b] Thierry Buffeteau,[c] Shaheen Pathan,[a,d] Shoji Nagaoka,[b,e] Emilie Pouget,[a] Sylvain Nlate,[a] Hirotaka Ihara,[d,e] and Reiko Oda*[a]

[a]Institute of Chemistry & Biology of Membranes & Nanoobjects (UMR5248 CBMN), CNRS - Université de Bordeaux - Bordeaux INP, 2 rue Robert Escarpit, 33607 Pessac, France

[b]Materials Development Department, Kumamoto Industrial Research Institute, 3-11-38 Higashimachi, Higashi-ku Kumamoto 862-0901, Japan

[c]Institut des Sciences Moléculaires (UMR5255 ISM), CNRS - Université de Bordeaux, 351 Cours de la Libération, 33405 Talence, France

[d]Department of Applied Chemistry and Biochemistry, Kumamoto University, 2-39-1 Kurokami, Chuo-ku Kumamoto 860-8555, Japan

[e]Kumamoto Institute for Photo-Electro Organics (PHOENICS), 3-11-38 Higashimachi, Higashi-ku Kumamoto 862-0901, Japan

Experimental details

Materials and instrumentations

All chemicals were of reagent grade and purchased from chemical suppliers. *N,N'*-Dihexadecyl-*N,N,N',N'*-tetramethylethylene diammonium L- (and D-) tartrate (16-2-16 L- (and D-) tartrate) were synthesized by the previously reported procedure[10]. Transmission electron microscopy (TEM) was performed with a JEM-1400plus (JEOL) at 80 kV for organic nanohelices and a CM120 (Filips) at 120 kV for silica-coated moleucular assembled nanohelices. ^{1}H-NMR spectra were recorded on an Avance II 300 MHz Spectrometer (BRUKER). Elemental analysis was performed with a vario MICRO cube Elemental analyzer (ELEMENTER). Thermal gravimetric analysis (TGA) was performed with a STA7200 (Hitachi High-tech Science). Circular dichroism (CD) and UV-visible absorption spectra were measured with a J-815 (JASCO). Circularly polarized luminescence (CPL) and fluorescence spectra were measured with a CPL-300 (JASCO). All spectra were measured using a quartz cell with 10 mm path length. To study about the chiral transfer mechanism (Figure 4), the scattering components of UV absorbance of L-helix-I were removed by peak decomposition using Voigt function (Figure S5). Carve fitting for CPL spectra was carried out using Voigt function. All CD, UV-visible and IR absorption, CPL, and fluorescence spectral measurements were carried out at 20 ˚C except for a temperature dependence studies.

Preparation of silica-coated molecular assembled nanohelices with various anions

5 mL of 16-2-16 L- (and D-) tartrate (1 mM) aqueous solution was heated at 60 ˚C to be clear solution. After cooled it down at 20 ˚C for 3 days, 5 mL of prehydrolyzed TEOS aqueous solution (TEOS : water = 1 : 20 v/v) containing 0.1 mM L- (and D-) tartaric acid was added to the 16-2-16 L- (and D-) tartrate aqueous solution and the mixture was kept at 20˚C for 18 hs. Unreacted TEOS was removed by washing with water at 4 ˚C using centrifuge (3000-4000*g*, 5 min.). Instead of water, 100 mM-KX (X = I, Br, Cl, F) aqueous solutions were used for the ion exchanging to obtain the silica-coated self-assembled nanohelices with halide ions (Hyb-helix-X). Excess of KX was removed by washing with water at 4 ˚C. Completion of each washing process was confirmed by weight of dried supernatent, UV-visible and ^{1}H-NMR spectra. Concentration of the obtained solutions was adjusted to be 2.0 mg mL^{-1} and kept at 4 ˚C for various spectral measurements.

Sample preparation for TEM observation

A drop (ca. 5 μL) of the sample solution was casted on the grid. The excess solution was removed by filter paper, and the grid was air-dried. The organic nanohelix were post stained with osmium tetroxide using an osmium plasma coater OPC60A (Filgen). After vacuum drying, these grids were used for TEM observation.

Infrared (IR) spectral measurements

In order to avoid the intense absorption peaks of H_2O in the 1500-1800 cm^{-1} and the 3000-4000 cm^{-1} regions, D_2O was used as a solvent for all IR spectral measurements. L-Hyb-helix-tart and L-Hyb-helix-X (X = I, Br, Cl, F) aqueous solutions (2.0 mg mL^{-1}) were washed with D_2O at 4 ˚C using centrifuge (10000*g*, 5 min.). The concentration of these samples was adjusted to be 20 mg mL^{-1}. All infrared spectra were recorded with a Thermo-Nicolet Nexus 670 FTIR spectrometer, at a resolution of 4 cm^{-1}, by coadding 50 scans. Samples were held in a demountable CaF_2 cell with fixed path length of 55 μm (Biotools™, Biotools). For the experiments with temperature variation, the cell was introduced in the BioJACK holder and the temperature was controlled by the Huber Ministat 125 refrigerated heating bath circulator. All IR spectra were shown with solvent absorption subtracted out.

Calculation of the occupancy of the space inside the silica walls

Theoretical weight percent of the space inside the silica walls (30.7 wt%) is calculated from the following values: The thickness of the silica wall (3.5 nm)[11c], the thickness of double bilayer membrane of gemini surfactants (6.5 nm)[9c],and densities of silica (2.2 g cm^{-1}) and double bilayer membrane of gemini surfactants (1.05 g cm^{-1})[9c]. The calculated value shows a good agreement of the experimental data of L-Hyb-helix-tart (29.4 wt%) and L-Hyb-helix-Br (30.0 wt%) obtained from TGA thermograms (Figure S3).

In-situ ion exchanging of L-Hyb-helix-Cl by adding KI

A certain volume (0-54 μL) of 10 mM-KI aqueous solution was added into 3.0 mL of L-Hyb-helix-Cl aqueous suspension (0.20 mg mL^{-1}) with stirring at 20 ˚C in the 10 mm quartz cell. The obtained mixture was used for the CD and UV absorption spectral measurements.

Preparation of L- and D-Hyb-helix-I_2

300 μL of 30%-H_2O_2 aqueous solution was added to 3 mL of L- (or D-) Hyb-helix-I aqueous suspension (0.20 mg mL^{-1}) with stirring at 20 ˚C in the 10 mm quartz cell. Obtained mixture was used for CD and UV absorption spectral measurements.

Preparation of L- and D-Hyb-helix-CuI

300 μL of L- (or D-) Hyb-helix-I aqueous suspension (2.0 mg mL^{-1}) was added to 3 mL of $CuSO_4$ aqueous solution (10 mM) with stilling at 20 ˚C in the 10 mm quartz cell. After adding 300 μL of KI aqueous solution (100 mM), obtained mixture was used for CPL and fluorescence spectral measurements.

Supplementary figures

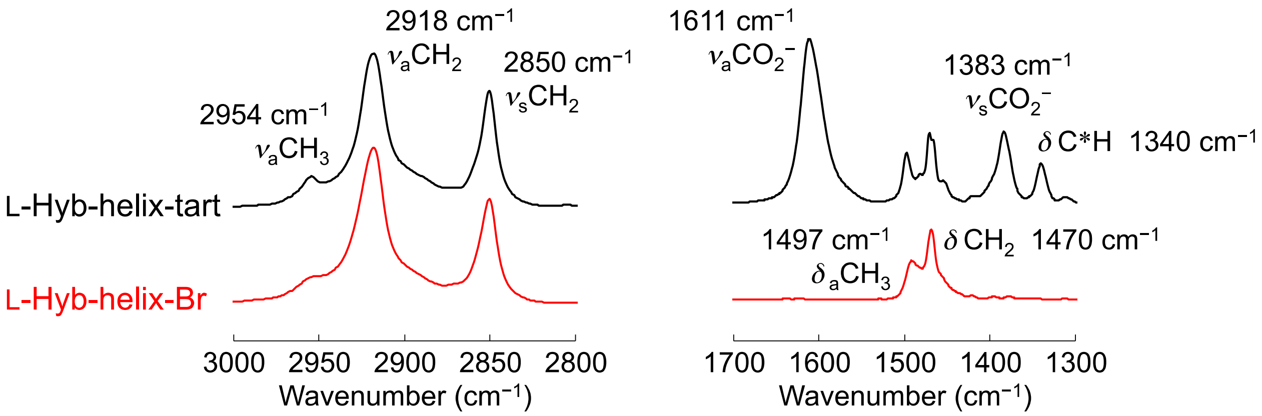

Figure S1 IR spectra of L-Hyb-helix-tart (black line) and L-Hyb-helix-Br (red line) in the 3000-2800 cm^{-1} (left) and 1700-1300 cm^{-1} regions (right). Concentration of silica-coated self-assembled nanohelices was 20 mg mL^{-1}. All spectra were measured in D_2O with a path length of 50 µm at 20 ˚C.

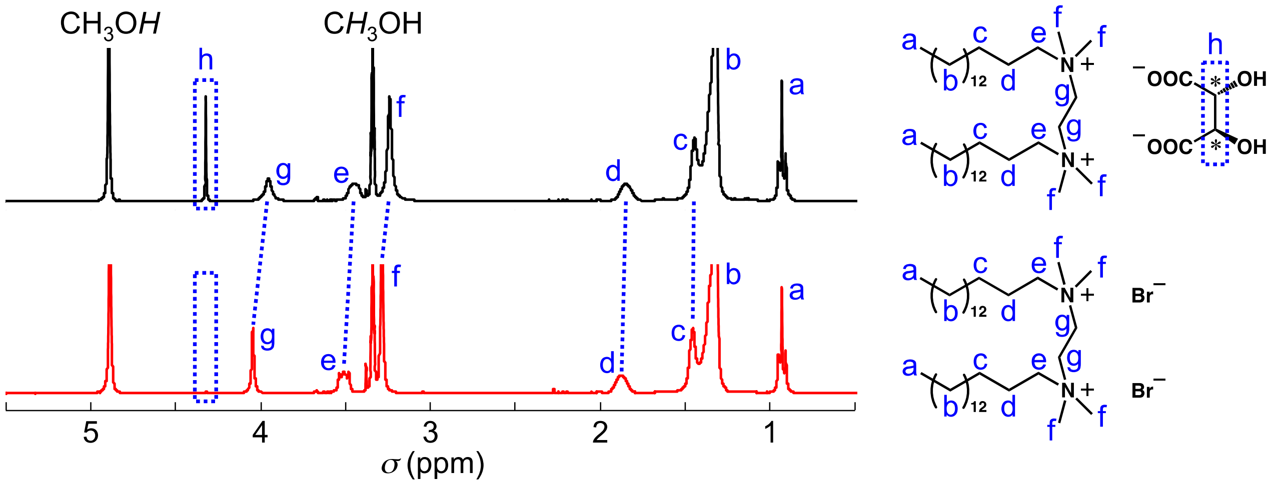

Figure S2 ^{1}H-NMR spectra of organic components extracted from L-Hyb-helix-tart (top) and L-Hyb-helix-Br (300 MHz, CD_3OD, room temperature).

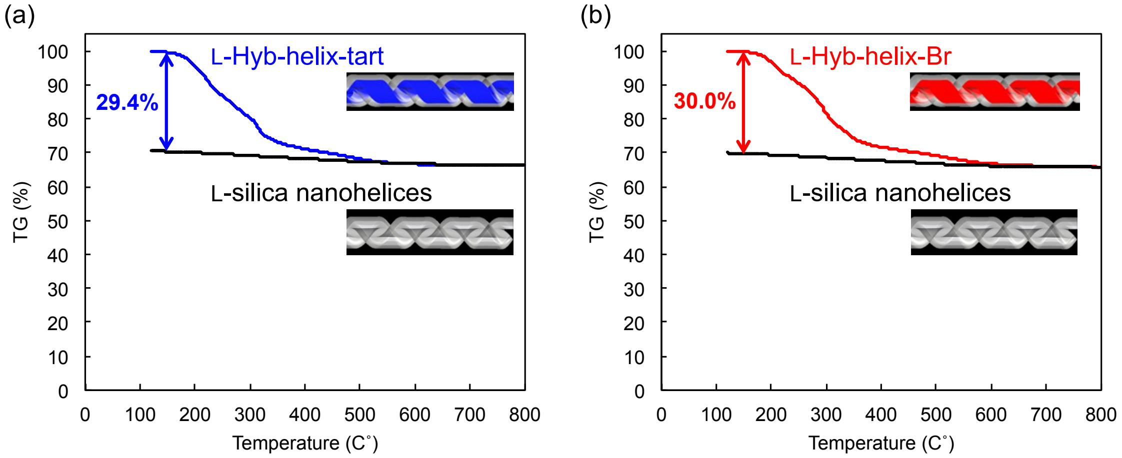

Figure S3 TGA thermograms of (a) L-Hyb-helix-tart and (b) L-Hyb-helix-Br. Black lines represent the TGA thermogram of silica-coated nanohelices after washed with methanol at 60 ˚C to remove all the organic components, which was confirmed by EA. All samples were heated (10 ˚C min^{-1}) from room temperature to 800 ˚C under air. Weight loss was calculated from the difference between the values of samples to L-silica nanohelices at 120 ˚C.

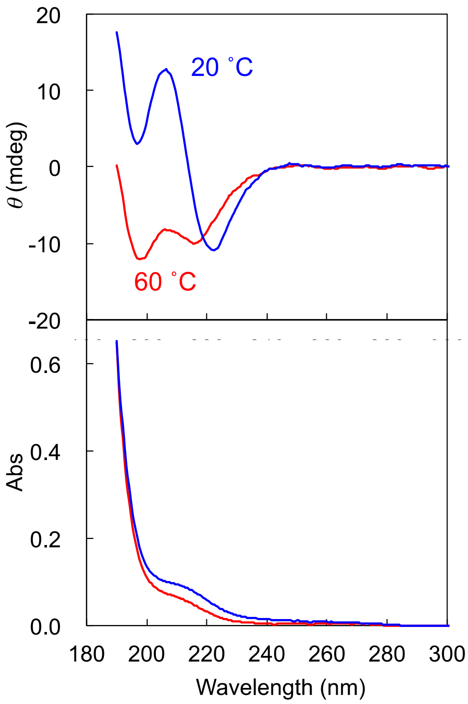

Figure S4 CD (top) and absorbance (bottom) spectra of 16-2-16 L-tartrate aqueous solution (1.0 mM) at 60 ˚C (red line) and 20 ˚C (blue line). These spectra were measured by using 1 mm quartz cell.

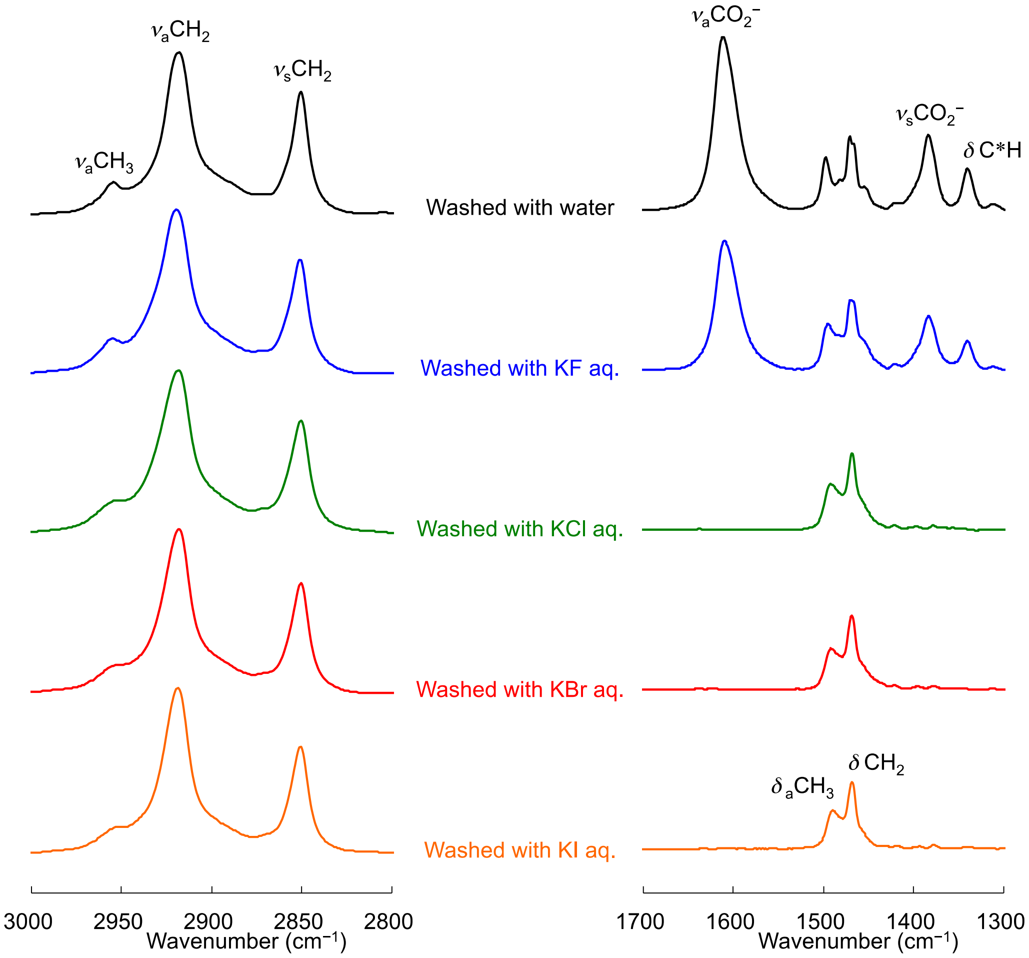

Figure S5 IR spectra of silica-coated self-assembled nanohelices after washing with water (black line) and 100 mM-KX (X = F, blue line; Cl, green line; Br, red line; I, orange line) aqueous solutions in the 3000-2800 cm^{-1} (left) and 1700-1300 cm^{-1} regions (right). Concentration of silica-coated self-assembled nanohelices was 20 mg mL^{-1}. All spectra were measured in D_2O with a path length of 50 µm at 20 ˚C.

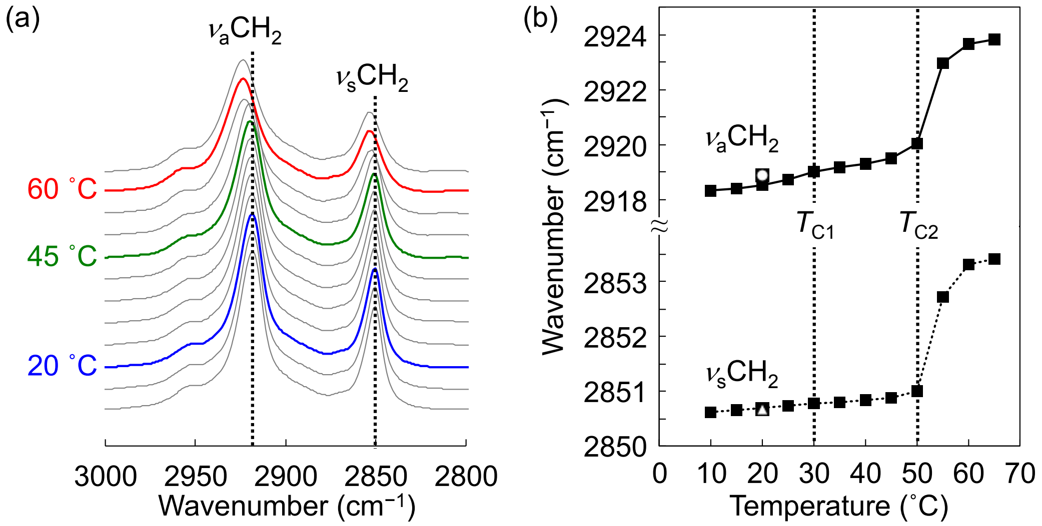

Figure S6 (a) IR spectra of L-Hyb-helix-I in D_2O at various temperatures from 10 ˚C (bottom) to 65 ˚C (top). (b) Temperature dependence of IR absorption of ν_aCH$_2$ and ν_sCH$_2$ bands.

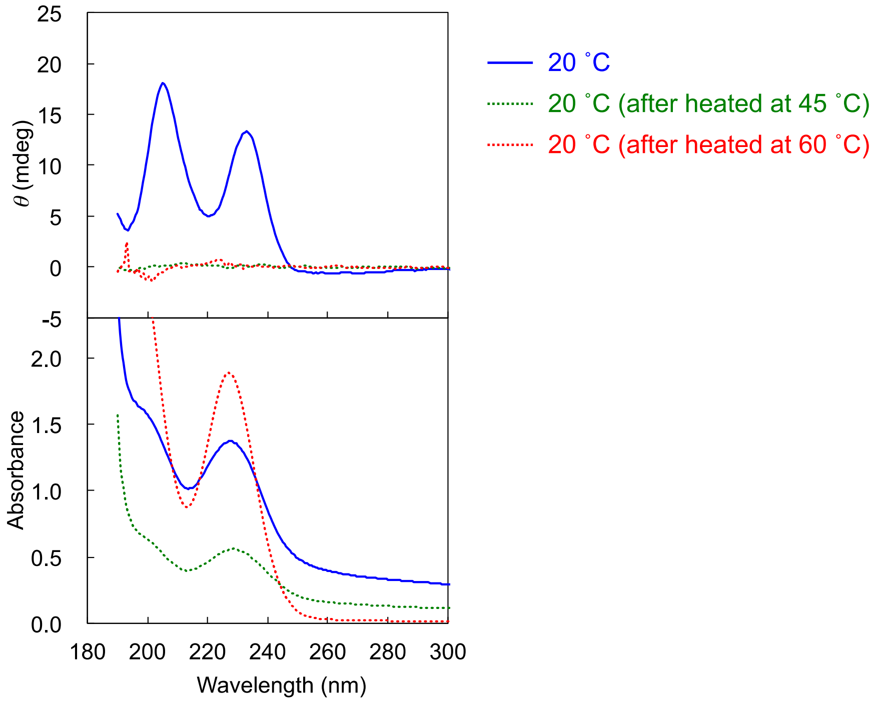

Figure S7 CD (top) and absorbance (bottom) spectra of L-Hyb-helix-I (0.20 mg mL^{-1}) in water at (20 ˚C, blue line; 20 ˚C after heated at 45 ˚C, green dotted line; 20 ˚C after heated at 60 ˚C, red dotted line).

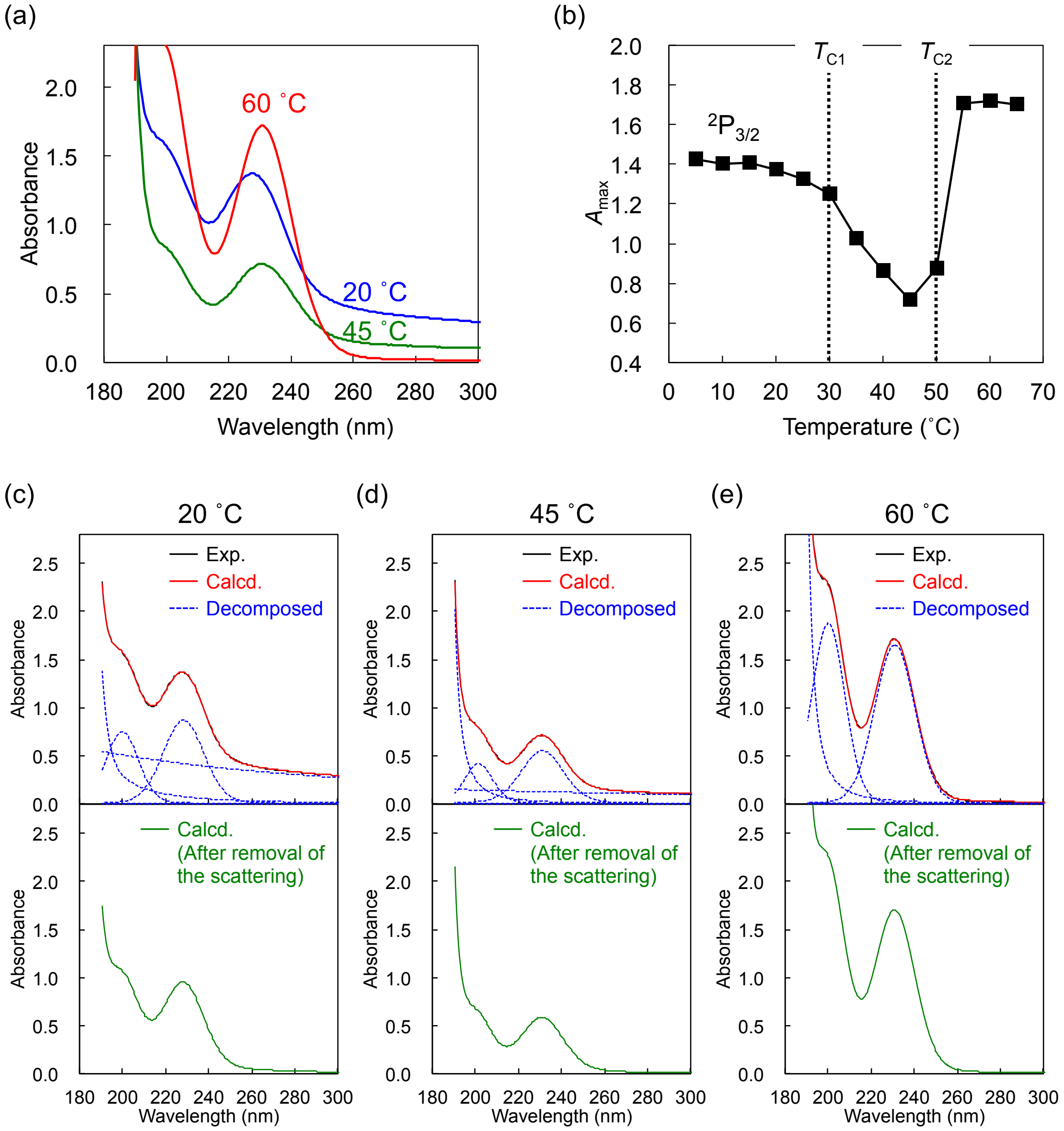

Figure S8 (a) UV absorption spectra of L-Hyb-helix-I (0.20 mg mL^{-1}) in water at 20 ˚C, 45 ˚C, and 60 ˚C without removal of the scattering component. (b) Temperature dependence of $^2P_{3/2}$ absorption without removal of the scattering component. UV absorption spectra of L-Hyb-helix-I (0.20 mg mL^{-1}) in water at (20 ˚C, (c); 45 ˚C, (d); 60 ˚C, (e)) before (top) and after (bottom) removal of the scattering component. Peak decomposition was carried out using Voigt function.

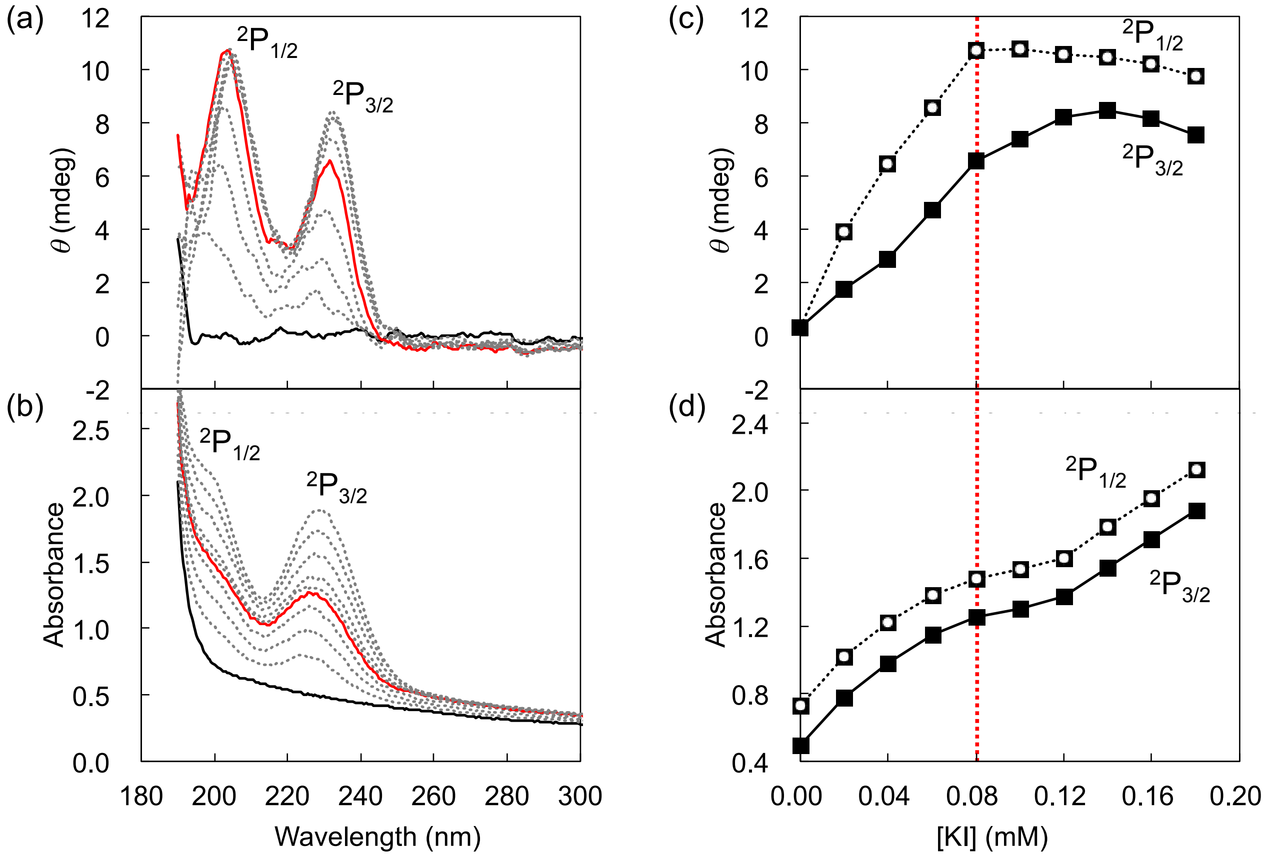

Figure S9 (a) CD and (b) UV absorption spectra of the L-hyb-helix-Cl (0.20 mg mL^{-1}) in various concentrations of KI (0-0.18 mM) in water at 20 ˚C. Effect of concentration of KI on (c) the ellipticities and (d) the UV absorption of $^2P_{1/2}$ and $^2P_{3/2}$ bands.

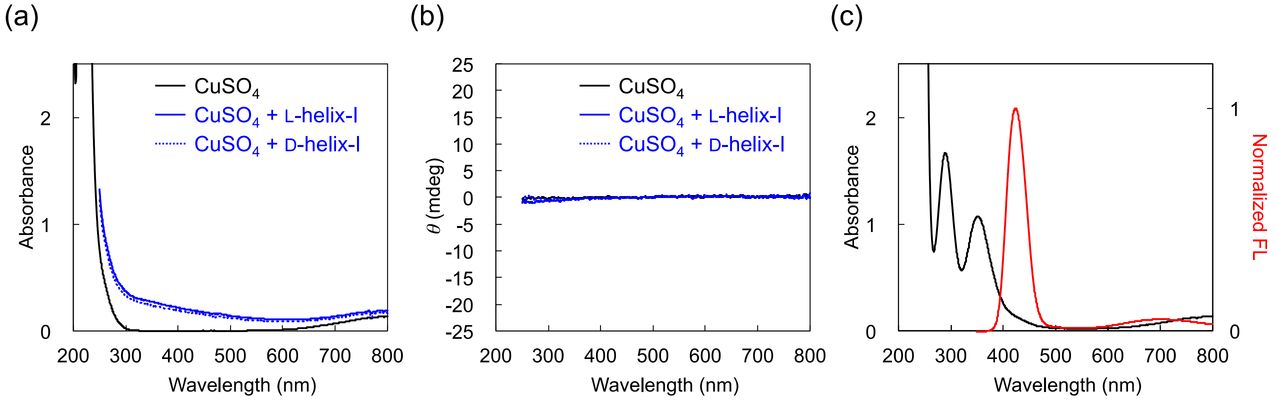

Figure S10 UV-visible absorption (a) and CD (b) spectra of $CuSO_4$ aqueous solutions before (black line) and after addition of L- (blue solid line) and D- (blue dotted line) Hyb-helix-I (0.20 mg mL^{-1}) at 20 ˚C. (c) UV-visible absorption (black line) and fluorescence (red line) spectra of the mixture of $CuSO_4$ and KI in water at 20 ˚C. [$CuSO_4$] = [KI] = 10 mM. The excitation wavelength was $\lambda = 290$ nm.